VSP

Advanced Robotics 25 (2011) 1697–1712

ADVANCED ROBOTICS
brill.nl/ar

Full paper

Dexterous Workspace Optimization of a Tricept Parallel Manipulator

Mir Amin Hosseini [a], **Hamid-Reza M. Daniali** [a,*] **and Hamid D. Taghirad** [b]

[a] Department of Mechanical Engineering, Babol University of Technology, Shariati Street, Babol, Iran

[b] Department of Electrical Engineering, K. N. Toosi University of Technology, Seyed Khandan, Tehran, Iran

Received 24 August 2010; accepted 12 November 2010

Abstract

The growing interest in the use of parallel manipulators in machining applications requires clear determination of the workspace and dexterity. In this paper, the workspace optimization of a Tricept parallel manipulator under joint constraints is performed. This parallel manipulator has complex degrees of freedom and, therefore, leads to dimensionally inhomogeneous Jacobian matrices. Here, we divide the Jacobian entries by units of length, thereby producing a new Jacobian that is dimensionally homogeneous. By multiplying the associated entries of the twist array to the same length, we made this array homogeneous as well. The workspace of the manipulator is parameterized using several design parameters and is optimized using a genetic algorithm. For the workspace of the manipulator, local conditioning indices and minimum singular values are calculated. For the optimal design, it is shown that by introducing the local conditioning indices and minimum singular values, the quality of the parallel manipulator is improved at the cost of workspace reduction.

Keywords

Tricept, singular value, dexterous workspace, complex degrees of freedom, parallel manipulator

1. Introduction

Parallel manipulators have received extensive attention over the last two decades. This popularity is due to the fact that they possess some specific advantages over their serial counterparts, such as stiffness, high accuracy and high load carrying capacity [1, 2]. One of the most famous parallel manipulators with machine tool application is the Tricept family, which has both rotational and translational de-

* To whom correspondence should be addressed. E-mail: mohammadi@nit.ac.ir

 DOI:10.1163/016918611X584640

grees of freedom (d.o.f.) [3]. In engineering applications, we often attach a great importance to the study of the dexterous workspace of a manipulator rather than the reachable workspace, especially for spatial parallel manipulators. The workspace of a manipulator is the domain of reach of its moving platform, which is bounded in the three-dimensional space. Moreover, kinetostatic performance or dexterity measures how well the system behaves with regard to force and motion transmission. Several dexterity criteria could be taken into account, such as service angle, manipulability, minimum singular values (MSVs), maximum singular values and condition number [4].

Most spatial parallel manipulators have complex d.o.f. This leads to dimensionally inhomogeneous Jacobian matrices [5]. Making the Jacobian matrices dimensionally homogeneous is very important when one deals with their singular values. Ranjbaran *et al.* [6] resolved this inconsistency by defining a characteristic length, by which they divided the Jacobian entries that have units of length, thereby producing a new Jacobian that is dimensionally homogeneous. Ma and Angeles [7] introduced another ratio called the natural length and used it for design optimization. Chablat *et al.* [8] used the characteristic length to determine the design parameter of a planar parallel mechanism with PRR chains to have an isotropic condition. Gosselin [9] introduced a method for formulating a dimensionally homogeneous Jacobian matrix for a planar mechanism with 1 rotational and 2 translational d.o.f. This Jacobian matrix relates the actuator velocities to the velocities of the x and y coordinates of two points on the moving platform. Kim and Ryu [10] furthered this work by using the velocities of three points on the moving platform to develop a dimensionally homogeneous Jacobian matrix. Pond and Carretero [11] furthered this method again by using three independent coordinates of three points on the moving platform. Moreover, Angeles [12] introduced the engineering characteristic length for a rigid body transformation matrix to make it homogeneous. Mansouri [13] used a power transition concept to make the Jacobian homogeneous.

Upon recalling the concept of characteristic length, we divide the Jacobian entries by units of length, thereby producing a new Jacobian that is dimensionally homogeneous. At the same time, we multiply the associated entries of the twist array by the same length, thereby producing a new twist array that is dimensionally homogeneous, as well. As this length makes a balance between linear and angular velocities of the twist array, we call it a weighting factor. Moreover, we will show that this weighting factor is position dependent for those methods that make the Jacobians homogenous differently [10, 11]. Furthermore, one can also assign different weighting factors to the different coordinates of the twist array with the same unit.

Parallel manipulators suffer from smaller workspaces relative to their serial counterparts; therefore, many researchers addressed the optimization of the workspace of parallel manipulators [14–16]. However, optimization for such a purpose might lead to a manipulator with poor dexterity. To alleviate this drawback some others considered both performance indices and volume of workspace si-

multaneously [17, 18]. Here, the workspace is parameterized using three design parameters, which are the moving and base platform radii and the upper part of the passive link length. Moreover, some geometric constraints are considered in the problem. Owing to the nonlinear discontinuous behavior of the problem, the genetic algorithm (GA) method is used here to optimize the workspace. For the workspace of the manipulator, local conditioning indices (LCI) and MSVs are calculated. Finally, the workspace is optimized by also considering these dexterity measures.

2. Tricept Mechanism

A Tricept robot, as depicted in Fig. 1, has 2 rotational and 1 translational d.o.f. [3]. The manipulator has three actuated limbs that connect the base to the moving platform. Each of these limbs consists of a spherical–prismatic–spherical (SPS) kinematic chain, where only the prismatic joint is actuated. Alternatively, one of the spherical joints can be replaced by a universal joint. Moreover, a passive prismatic–universal (PU) limb connects the center of the moving platform to the base. We attach frames $\{P(uvw)\}$ and $\{O(xyz)\}$ to the moving and base platforms, respectively. When the moving platform is parallel to the base, the two revolute axes of the universal joints of the center passive leg are parallel with the base frame's x- and y-axes, respectively.

Siciliano [19] studied the kinematics and manipulability of Tricept. Pond and Carretero [20] formulated its square dimensionally homogeneous Jacobian matrices based on three independent coordinates of three nodes of the moving platform. Architectural optimization of Tricept was studied by Zhang and Gosselin [21]. They used the GA method to optimize the stiffness and moving platform accuracy. Here,

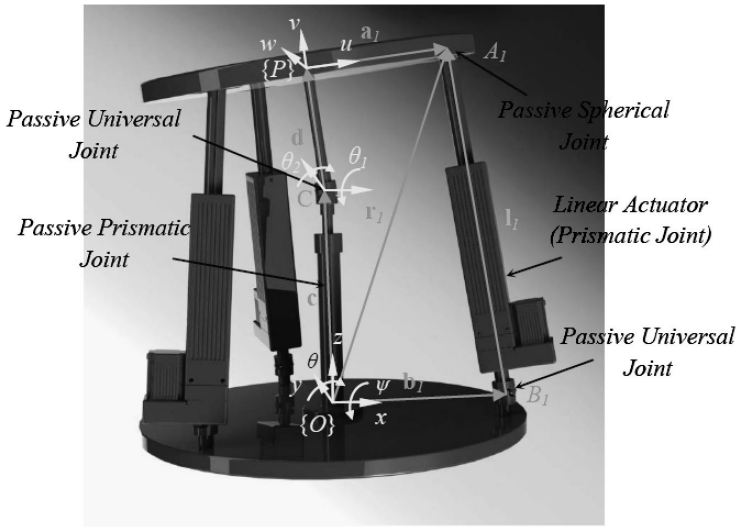

Figure 1. Tricept structure and geometric model.

we use the weighting factor method, analytical method and a numerical search to calculate the workspace. Moreover, we use the GA method to optimize the dexterous workspace of the Tricept robot.

2.1. Velocity Analysis

The geometric model of the manipulator is depicted in Fig. 1. The closure equation for the ith leg can be written as:

$$\mathbf{c} + \mathbf{R}(\mathbf{a}_i + \mathbf{d}) = b_i \mathbf{n}_{\mathrm{b}i} + l_i \mathbf{n}_{\mathrm{l}i}, \tag{1}$$

where $\mathbf{c}$ and $\mathbf{d}$ are the vectors from O to C and C to P, respectively. $\mathbf{R}$ is rotation matrix carrying frame $\{P\}$ into an orientation coincident with that of frame $\{O\}$; $\mathbf{a}_i$ is the position vector from P to A_i in frame $\{P\}$; $\mathbf{b}_i$ is the position vector of point B_i in the global frame. Moreover, $\mathbf{n}_{\mathrm{b}i}$ and $\mathbf{n}_{\mathrm{l}i}$ are the unit vectors showing the directions of vectors $\mathbf{b}_i$ and $\mathbf{l}_i$, respectively.

Taking the first time derivative of (1) yields:

$$\dot{\mathbf{c}} + \boldsymbol{\omega}_{\mathrm{p}} \times (\mathbf{R}(\mathbf{a}_i + \mathbf{d})) = \dot{l}_i \mathbf{n}_{\mathrm{l}i} + \boldsymbol{\omega}_{\mathrm{l}} \times l_i \mathbf{n}_{\mathrm{l}i}, \tag{2}$$

where $\boldsymbol{\omega}_{\mathrm{p}}$ and $\boldsymbol{\omega}_{\mathrm{l}}$ are the angular velocity vectors of the moving platform and the limb, respectively. The inner product of the both sides of (2) by $\mathbf{n}_{\mathrm{l}i}$ upon simplification leads to:

$$\mathbf{n}_{\mathrm{l}i}\dot{\mathbf{c}} + \mathbf{n}_{\mathrm{l}i}\boldsymbol{\omega}_p \times (\mathbf{R}(\mathbf{a}_i + \mathbf{d})) = \dot{l}_i. \tag{3}$$

Writing (3), for $i = 1, \ldots, 3$, in the following form yields:

$$\mathbf{J}\dot{\mathbf{x}} = \dot{\mathbf{q}}, \tag{4}$$

where $\dot{\mathbf{x}}$ is the three-dimensional (3-D) twist vector, $\dot{\mathbf{q}}$ is the 3-D actuator velocity vector and $\mathbf{J}$ is the Jacobian matrix:

$$\dot{\mathbf{x}} = [\,\dot{c} \quad \dot{\psi} \quad \dot{\theta}\,]^{\mathrm{T}} \tag{5}$$

$$\dot{\mathbf{q}} = [\,\dot{l}_1 \quad \dot{l}_2 \quad \dot{l}_3\,]^{\mathrm{T}} \tag{6}$$

$$\mathbf{J} = \begin{bmatrix} n_{\mathrm{l}1z} & (\mathbf{R}(\mathbf{a}_1 + \mathbf{d}) \times \mathbf{n}_{\mathrm{l}1})_x & (\mathbf{R}(\mathbf{a}_1 + \mathbf{d}) \times \mathbf{n}_{\mathrm{l}1})_y \\ n_{\mathrm{l}2z} & (\mathbf{R}(\mathbf{a}_2 + \mathbf{d}) \times \mathbf{n}_{\mathrm{l}2})_x & (\mathbf{R}(\mathbf{a}_2 + \mathbf{d}) \times \mathbf{n}_{\mathrm{l}2})_y \\ n_{\mathrm{l}3z} & (\mathbf{R}(\mathbf{a}_3 + \mathbf{d}) \times \mathbf{n}_{\mathrm{l}3})_x & (\mathbf{R}(\mathbf{a}_3 + \mathbf{d}) \times \mathbf{n}_{\mathrm{l}3})_y \end{bmatrix}. \tag{7}$$

3. Workspace Analysis

There are several methods (geometrical [22], analytical and numerical [23]) to analyze the workspace of manipulators. In this section, we study the workspace of a Tricept manipulator based on a combination of analytical and numerical methods.

- *Algorithm*. In order to generate the workspace of a Tricept parallel manipulator, we divide the three dimensional ψ–θ–Z workspace of the moving platform into a series of subworkspaces that are parallel to the ψ–θ plane. Then a numerical searching method is adopted to determine the boundary of the subworkspaces.

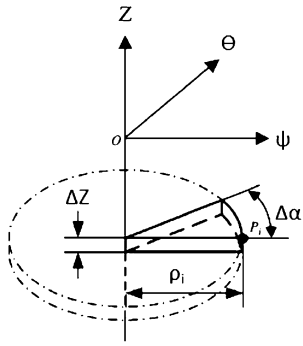

Figure 2. Boundary points of a subworkspace.

Finally, the volume of the workspace is calculated quantitatively. The searching method adopted here is similar to the one used in Ref. [24].

In the particular subworkspace at elevation Z_i (within the workspace), to determine the boundary of the subworkspace one may find trajectories formed by the end of polar vector $\boldsymbol{\rho}_i$ rotating about the z-axis from 0 to 2π (Fig. 2). When the boundary point in the direction of $\boldsymbol{\rho}_i$ is found as $P_i(\rho\cos\alpha, \rho\sin\alpha, Z_i)$, where ρ_i is the distance between Z_i and P_i, α will be increased by $\Delta\alpha$ and the next point will be found, similarly. The determination of point P_i is based on the inverse kinematics of the Tricept. When searching the next boundary point P_{i+1}, we set the initial value of ρ_{i+1} as ρ_i and judge whether point P_{i+1} is in the range of the workspace; if yes, then increase ρ_{i+1}, if not, then decrease ρ_{i+1} until point P_{i+1} is on the boundary of the workspace. Once the boundary points in the subworkspace are all searched out, Z_i will be decreased by ΔZ and the new search will be performed again. Moreover, when α is increased by $\Delta\alpha$, the unit volume of the corresponding workspace can be expressed approximately as:

$$\mathrm{d}V = \frac{\Delta\alpha}{2\pi}\pi\rho_i^2\Delta Z. \tag{8}$$

Therefore, the volume of the workspace can be calculated as:

$$V = \sum_{Z_i=Z_{\min}}^{Z_{\max}} \sum_{\alpha=0}^{2\pi} \frac{1}{2}\rho_i^2\Delta\alpha\Delta Z. \tag{9}$$

- *Geometric constraints*. There are some geometric constraints in the design process. These constraints include upper and lower limits of actuators, spherical and universal joints, links lengths and platforms radii. It is simple to calculate the cone angle of joints (ζ) by using the geometric relations between actuator vector and the moving platform pose. The geometric constraints of the Tricept robot are given in Table 1.

Table 1.
Geometric constraints of the Tricept manipulator

Actuator (mm)	ζ (deg)	d (mm)	r_b (mm)	r_a (mm)
400–750	±60	0–200	300–500	200–300

- *Design constraints*. These constraints include all the expected performances of the design process, such as stiffness, dexterity, etc. Condition number is quite often used as an index to describe the dexterity of a robot and the distance of a pose from a singularity. The condition number also measures the magnitude of the relative error of the wrench introduced by the relative error in joint torques and reflects the sensitivity of the wrench due to joint torque error. Similarly, the use of minimum allowable singular value restricts the workspace to poses where the manipulator moves at a minimum allowable speed. The advantage in this region is that the resolution over the moving platform pose is finer. Here, we optimized Tricept for dexterity measures, namely the condition number as a LCI and the MSV.

3.1. Weighting Factor or Points Based Method

Condition numbers and MSVs of the Jacobian matrices are known as a kinetostatic performance indices of parallel manipulators [7, 25]. Indeed, in order to determine the condition number and MSV of the Jacobian matrices, we must order their singular values from largest to smallest. However, in the presence of positioning and orienting tasks, three of these singular values (i.e., those associated with positioning) are dimensionless, while those associated with orientation have units of length, thereby making such an ordering impossible. This dimensional inhomogeneity can be resolved by a weighting factor.

Dividing the second and the third columns of the Jacobian matrix of (7) by a length and multiplying the second and the third coordinates of the twist vector to the same length leads to the following dimensionally homogeneous relation:

$$\begin{bmatrix} n_{11z} & \frac{(\mathbf{R}(\mathbf{a}_1+\mathbf{d})\times n_{11})_x}{l} & \frac{(\mathbf{R}(\mathbf{a}_1+\mathbf{d})\times n_{11})_y}{l} \\ n_{12z} & \frac{(\mathbf{R}(\mathbf{a}_2+\mathbf{d})\times n_{12})_x}{l} & \frac{(\mathbf{R}(\mathbf{a}_2+\mathbf{d})\times n_{12})_y}{l} \\ n_{13z} & \frac{(\mathbf{R}(\mathbf{a}_3+\mathbf{d})\times n_{13})_x}{l} & \frac{(\mathbf{R}(\mathbf{a}_3+\mathbf{d})\times n_{13})_y}{l} \end{bmatrix} \begin{bmatrix} \dot{c} \\ l\dot{\psi} \\ l\dot{\theta} \end{bmatrix} = \begin{bmatrix} \dot{l}_1 \\ \dot{l}_2 \\ \dot{l}_3 \end{bmatrix}. \tag{10}$$

Physically, this implies some sort of tradeoff between position and orientation components of the twist vector. This weighting factor should be constant throughout the workspace. Moreover, one might compare one unit of the linear velocity with $m \times l$ units of angular velocity around the x-axis and $n \times l$ units of angular velocity

around the y-axis. Thus, we can assign different weighting factors to the different coordinates of the twist vector:

$$\begin{bmatrix} n_{11z} & \frac{(\mathbf{R}(\mathbf{a}_1+\mathbf{d})\times n_{11})_x}{lm} & \frac{(\mathbf{R}(\mathbf{a}_1+\mathbf{d})\times n_{11})_y}{ln} \\ n_{12z} & \frac{(\mathbf{R}(\mathbf{a}_2+\mathbf{d})\times n_{12})_x}{lm} & \frac{(\mathbf{R}(\mathbf{a}_2+\mathbf{d})\times n_{12})_y}{ln} \\ n_{13z} & \frac{(\mathbf{R}(\mathbf{a}_3+\mathbf{d})\times n_{13})_x}{lm} & \frac{(\mathbf{R}(\mathbf{a}_3+\mathbf{d})\times n_{13})_y}{ln} \end{bmatrix} \begin{bmatrix} \dot{c} \\ lm\dot{\psi} \\ ln\dot{\theta} \end{bmatrix} = \begin{bmatrix} \dot{l}_1 \\ \dot{l}_2 \\ \dot{l}_3 \end{bmatrix}. \tag{11}$$

Pond and Carretero [11] have shown the kinematic equation as:

$$\mathbf{J_d}\dot{\mathbf{X}}'' = \dot{\mathbf{q}}, \tag{12}$$

where $\mathbf{J_d}$ is dimensionless Jacobian matrix and $\dot{\mathbf{X}}''$ is a vector of the z coordinate velocity of three points of a moving platform which is given as:

$$\dot{\mathbf{X}}'' = [\, \dot{A}_{1z} \;\; \dot{A}_{2z} \;\; \dot{A}_{3z} \,]^{\mathrm{T}}, \tag{13}$$

in which the components are functions of the moving platform pose coordinates, according to:

$$\dot{A}_{1z} = \dot{c} + \dot{\psi}(-d\sin\psi\cos\theta) + \dot{\theta}(-d\sin\theta\cos\psi - r_{\mathrm{a}}\cos\theta) \tag{14}$$

$$\begin{aligned} \dot{A}_{2z} = \dot{c} &+ \dot{\psi}\begin{pmatrix} -d\sin\psi\cos\theta \\ +\, r_{\mathrm{a}}\cos\psi\cos\theta\sin\alpha \end{pmatrix} \\ &+ \dot{\theta}\begin{pmatrix} -d\sin\theta\cos\psi - r_{\mathrm{a}}\cos\theta\cos\alpha \\ -\, r_{\mathrm{a}}\sin\theta\sin\psi\sin\alpha \end{pmatrix} \end{aligned} \tag{15}$$

$$\begin{aligned} \dot{A}_{3z} = \dot{c} &+ \dot{\psi}\begin{pmatrix} -d\sin\psi\cos\theta \\ +\, r_{\mathrm{a}}\cos\psi\cos\theta\sin\beta \end{pmatrix} \\ &+ \dot{\theta}\begin{pmatrix} -d\sin\theta\cos\psi - r_{\mathrm{a}}\cos\theta\cos\beta \\ -\, r_{\mathrm{a}}\sin\theta\sin\psi\sin\beta \end{pmatrix}. \end{aligned} \tag{16}$$

Consequently, (12) can be written as:

$$\mathbf{J_d}\mathbf{D}\dot{\mathbf{x}} = \dot{\mathbf{q}}, \tag{17}$$

where:

$$\mathbf{D}_{3\times 3} = \begin{bmatrix} 1 & p_1 & t_1 \\ 1 & p_2 & t_2 \\ 1 & p_3 & t_3 \end{bmatrix}, \tag{18}$$

in which:

$$p_1 = -d\sin\psi\cos\theta \tag{19}$$

$$p_2 = -d\sin\psi\cos\theta + r_{\mathrm{a}}\cos\psi\cos\theta\sin\alpha \tag{20}$$

$$p_3 = -d\sin\psi\cos\theta + r_{\mathrm{a}}\cos\psi\cos\theta\sin\beta \tag{21}$$

$$t_1 = -d\sin\theta\cos\psi - r_{\mathrm{a}}\cos\theta \tag{22}$$

$$t_2 = -d\sin\theta\cos\psi - r_{\mathrm{a}}\cos\theta\cos\alpha - r_{\mathrm{a}}\sin\theta\sin\psi\sin\alpha \tag{23}$$

$$t_3 = -d\sin\theta\cos\psi - r_{\mathrm{a}}\cos\theta\cos\beta - r_{\mathrm{a}}\sin\theta\sin\psi\sin\beta. \tag{24}$$

Table 2.
Parameters of the Tricept design

Actuator stroke (mm)	Actuator minimum length (mm)	C stroke (mm)	d (mm)	r_b (mm)	r_a (mm)
350	400	200–400	200	500	200

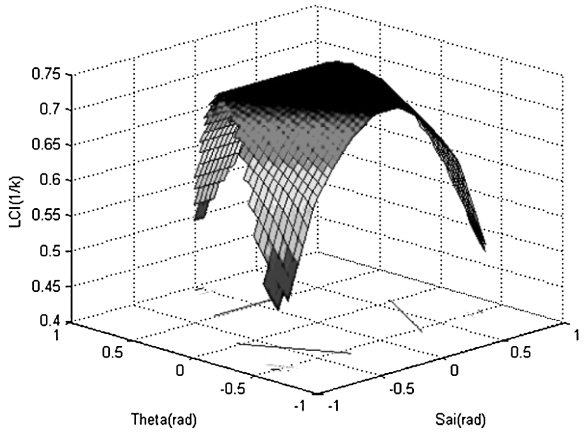

Figure 3. Loci of LCI at $z = 500$ mm with a weighting factor equal to 200 mm.

Pond and Carretero [11] evaluated the MSV and condition index of $\mathbf{J_d}$, while others, including the present study, consider the conditioning of Jacobian matrix $\mathbf{J_dD}$. It is noteworthy that the relation between joint rates and twist vector is of great interest in kinetostatic analysis. Therefore, considering the conditioning of $\mathbf{J_d}$ bears no physical meaning and one should always consider the conditioning of $\mathbf{J_dD}$. Moreover, they explicitly considered some weighting factors, namely those singular values of $\mathbf{D}$ that are obviously pose dependent. Thus, using a predefined weighting factor, as suggested in the present study, leads to a homogeneous Jacobian whose conditioning has immediate physical meaning. In the following, a design of a Tricept as given in Table 2 is considered. The LCI of the homogeneous Jacobian with a weighting factor equal to 200 at $z = 500$ mm is depicted in Fig. 3. Moreover, the LCI of the homogeneous Jacobian according to the point based method at the same elevation is depicted in Fig. 4. One can see the obvious differences between the plotted LCIs. Those points with higher LCI, based on the first method, have a poor LCI according to the second method and *vice versa*.

4. GA Optimization

One of the drawbacks of parallel manipulators is their limited workspaces. It is more limited in the presence of constraints such as dexterity, isotropy and joints

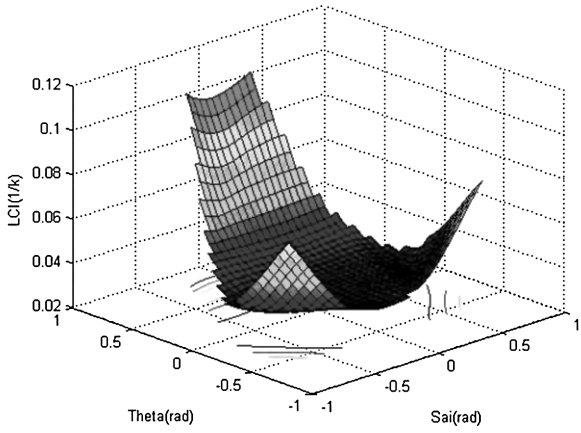

Figure 4. Loci of LCI at $z = 500$ mm by point coordinates-based formulation.

limits. Clearly, the optimal design problem is a constrained nonlinear optimization problem. Here, we resort to a direct search method; namely GA, which has been widely studied as a global optimization technique [26, 27]. The algorithm is robust (i.e., it normally works regardless of irregularities of the objective function).

4.1. Setup of the GA Optimization

4.1.1. Design Variables

There are three parameters to be optimized to define the manipulator architecture: the moving and base platform radii (r_a and r_b), and the upper part of middle link length (d), whose limitations are given in Table 1.

4.1.2. GA Parameters Setup

In order to apply the GA for optimization, six fundamental issues are required to be determined: chromosome representation, selection function, genetic operators, population size, termination criteria and evaluation function [28].

The chromosome representation of the GA is mainly classified into three categories of binary representation, gray representation and real number representation, known as float point representation. Like most applications of the GA to constrained optimization problems, the float point representation, which is encoded as a vector of real numbers to represent a solution, is adopted for the problem at hand. Here, the normalized geometric selection is adopted, and the non-uniform mutation and arithmetic crossover are selected as genetic operators, as well.

The population size determines the number of individuals in the population at each generation and the size is set to be 50 in the current optimization. The most frequently used termination criteria is a specified maximum number of generations. The maximum number of generations is chosen as 100. Moreover, the objective functions are chosen as the evaluation functions.

5. Case Study

5.1. Maximum Workspace Volume with Geometric Constraints

Here, the workspace is parameterized using three design parameters, which are the moving and base platform radii (r_a and r_b) and the upper part of passive link length (d), all summarized in the following vector:

$$\boldsymbol{\lambda} = [r_a, r_b, d]^T. \tag{25}$$

Then, using the GA method, the workspace is optimized subject to some geometric constraints as given in Table 1.

Therefore, our optimization problem yields:

$$V^* = \mathrm{Max}(V(d, r_a, r_b)), \tag{26}$$

subject to:

(i) $200 < r_a < 300$, $300 < r_b < 500$, $20 < d < 200$;

(ii) $400 <$ actuator length $(L) < 750$, $-60 < \zeta_i < 60$ deg.

Solving this optimization problem by the GA leads to the data given in Table 3, in which the maximum workspace is 944.2176 (mm · rad^2). Moreover, this workspace is illustrated in Fig. 5.

Table 3.
Maximum workspace volume with geometric constraints

No. of iterations	V^* (mm · rad^2)	d (mm)	r_b (mm)	r_a (mm)
51	944.2176	20	300.062	200

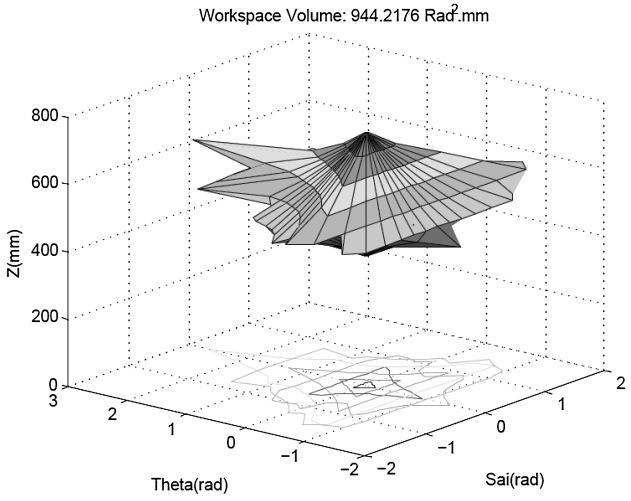

Figure 5. Maximum workspace volume with geometric constraints.

5.2. Constraint Evaluation

In the following, we evaluate non-geometric constraints (i.e., MSV and LCI) for different elevation ranges of the foregoing manipulator. MSV and LCI for different elevation ranges are depicted in Figs 6 and 7, respectively.

Moreover, the workspace volume of the manipulator *versus* the minimum permissible limit on singular values is depicted in Fig. 8. As the minimum permissible limit on singular values is reduced, the dexterous workspace continues to be reduced and vanishes at the minimum permissible limit on a singular value equal to 1.21. Moreover, the workspace volume of the manipulator *versus* the minimum permissible limit on the LCI is depicted in Fig. 9. As the minimum permissible limit on the LCI is reduced, the dexterous workspace continues to be reduced and vanishes at the minimum permissible limit of the LCI equal to 0.71.

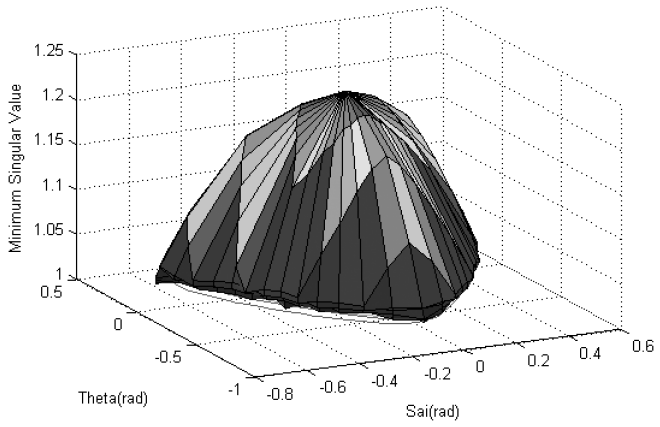

Figure 6. MSV for different elevations (from lower, 275 mm to upper, 775 mm).

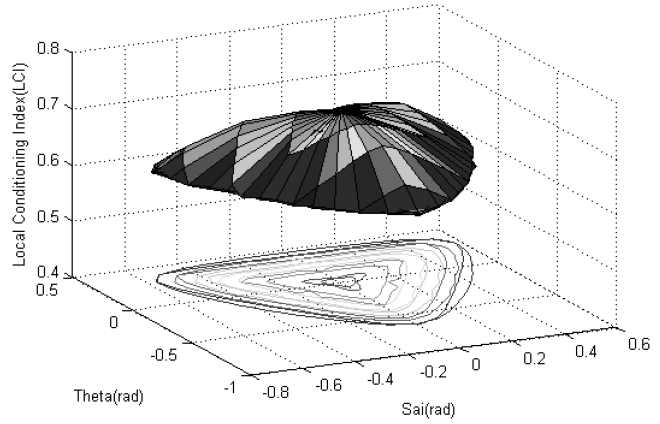

Figure 7. LCI for different elevations (from lower, 275 mm to upper, 775 mm).

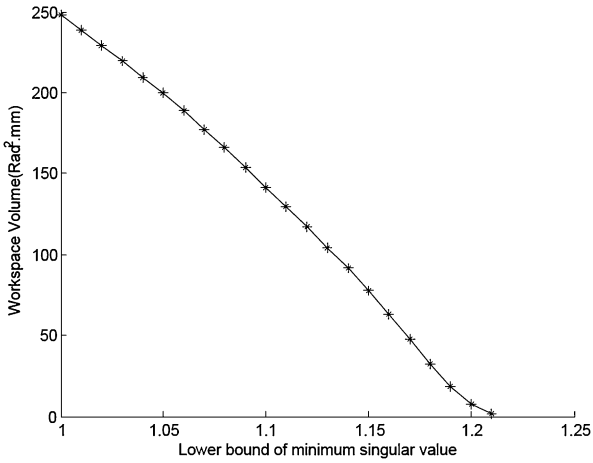

Figure 8. Workspace volume variation *versus* the minimum permissible limit on singular values.

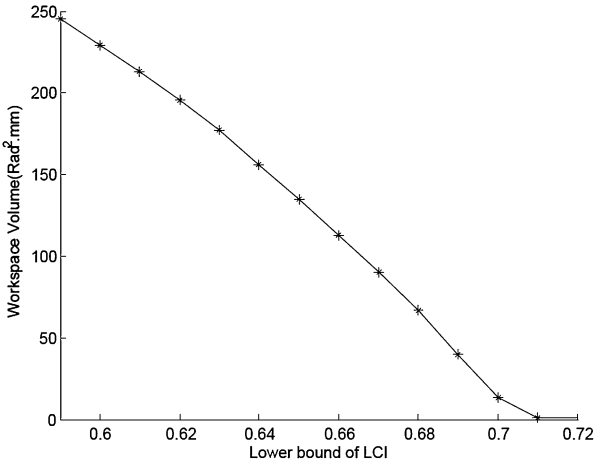

Figure 9. Workspace volume variation *versus* the minimum permissible limit on the LCI.

5.3. Dexterous and High Velocity Workspace Volume

Dexterous and high velocity workspaces are subworkspaces of the reachable workspace of Fig. 5. Considering any minimum permissible limit on singular values leads to the workspace with a lower bound for moving platform velocities, while considering the minimum permissible limit on the LCI leads to the manipulator as close as to isotropic conditions. For the workspace of the manipulator, depicted in Fig. 5, considering the minimum permissible limit on the LCI to be greater than or equal to 0.6 and the MSV to be greater than or equal to 1 yields the workspace of Fig. 10, with the volume of 269.2702 $\text{rad}^2 \cdot \text{mm}$. This volume of workspace is 72.5% less than the volume without considering these constraints.

In the following, the workspace volume of the Tricept is optimized by constraining the MSV and LCI of the Jacobian matrix to be within the defined ranges along

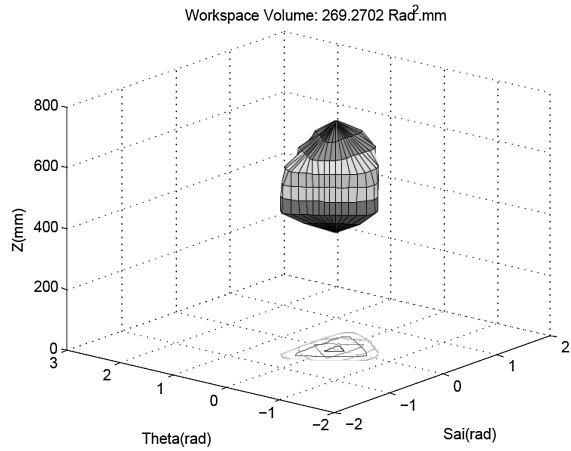

Figure 10. Subworkspace of the maximum workspace by limiting the MSV and LCI.

Table 4.
Optimization results for the design constrained workspace

No. of iterations	W^* (mm · rad^2)	d (mm)	r_b (mm)	r_a (mm)
52	363.9267	98.974	379.508	211.949

with the geometric constraints of Table 1. Therefore, the optimization problem can be rewritten as:

$$W^* = \text{Max}(V(d, r_a, r_b)), \tag{27}$$

subject to:

(i) LCI $\geqslant 0.6$;

(ii) $\sigma_{\min} \geqslant 1$;

(iii) $200 < r_a < 300$, $300 < r_b < 500$, $20 < d < 200$;

(iv) $400 <$ actuator length $(L) < 750$, $-60 < \zeta_i < 60$ deg.

Items (i) and (ii) represent the design constraints, while items (iii) and (iv) represent the geometric constraints. Solving this problem by the GA leads to the data given in Table 4, in which the maximum workspace is 363.9267 mm·rad^2, 35.1% more than that volume of Fig. 10. This workspace is illustrated in Fig. 11.

Moreover, the convergence of the algorithm is very fast and it is shown in Fig. 12.

6. Conclusions

In this paper the workspace optimization of a Tricept has been performed. This parallel manipulator has complex d.o.f. and, therefore, leads to dimensionally inhomogeneous Jacobian matrices. Here, some entries of the Jacobian have been divided

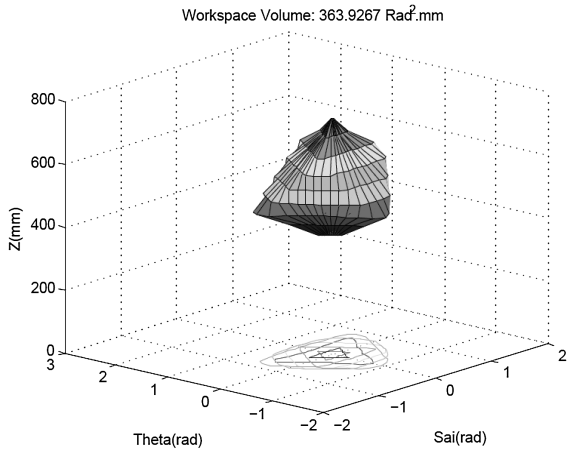

Figure 11. Maximum dexterous workspace.

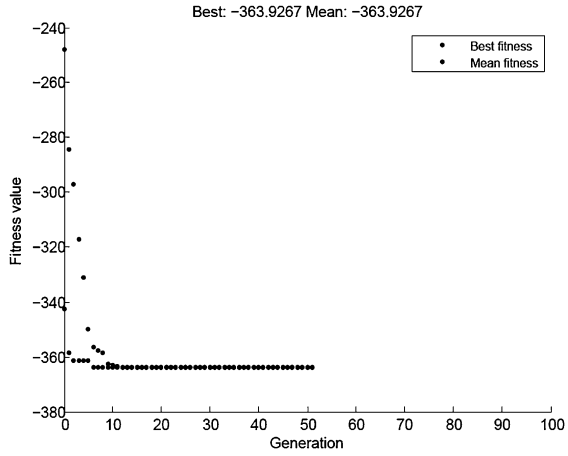

Figure 12. Convergence of optimization procedure.

by units of length, thereby producing a new Jacobian that is dimensionally homogeneous. By multiplying the associated entries of the twist array to the same length, this array has been made homogeneous as well. As this length makes a balance between linear and angular velocities of the twist array, we have called it a weighting factor. It was illustrated that the weighting factor method was more reliable than the other methods. Moreover, for the platform, the workspace has been parameterized using three design parameters, which were the moving and base platform radii and the upper part of the passive link length. Then, using the GA method, the workspace has been optimized subject to some geometric constraints. Furthermore, two workspace performance indices (i.e., LCI and MSVs) have been calculated for the workspace of the manipulator. Finally, it has been shown that by introducing the LCI and MSVs, the quality of the parallel manipulator was improved at the cost of workspace reduction.

References

1. J.-P. Merlet, *Parallel Robots*. Springer, Berlin (2006).
2. O. Masory and J. Wang, Workspace evaluation of Stewart platforms, *Adv. Robotics J.* **9**, 443–461 (1995).
3. K.-E. Neumann, US Patent 4,732,525 (1988).
4. C. Gosselin and J. Angeles, A global performance index for the kinematic optimization of robotic manipulators, *J. Mech. Des.* **113**, 220–226 (1991).
5. J. A. Carretero, R. P. Podhorodeski, M. A. Nahon and C. M. Gosselin, Kinematic analysis and optimization of a new three degree-of-freedom spatial parallel manipulator, *J. Mech. Des.* **122**, 17–24 (2000).
6. F. Ranjbaran, J. Angeles, M. A. Gonzalez-Palacios and R. V. Patel, The mechanical design of a seven-axes manipulator with kinematic isotropy, *J. Intell. Robotic Syst.* **14**, 21–41 (1995).
7. O. Ma and J. Angeles, Optimum architecture design of platform manipulators, in: *Proc. IEEE Int. Conf. on Advanced Robotics*, Pisa, pp. 1130–1135 (1991).
8. D. Chablat, P. Wenger, S. Caro and Angeles, The iso-conditioning loci of planar three d.o.f. parallel manipulators, in: *Proc. ASME Design Engineering Technical Conf.*, Montreal, CD-ROM DETC2002/MECH-34268 (2002).
9. C. M. Gosselin, The optimum design of robotic manipulators using dexterity indices, *J. Robotics Autonomous Syst.* **9**, 213–226 (1992).
10. S.-G. Kim and J. Ryu, New dimensionally homogeneous Jacobian matrix formulation by three end-effector points for optimal design of parallel manipulators, *IEEE Trans. Robotics Automat.* **19**, 731–737 (2003).
11. G. Pond and J. A. Carretero, Quantitative dexterous workspace comparison of parallel manipulators, *Mech. Mach. Theory* **42**, 1388–1400 (2007).
12. J. Angeles, Is there a characteristic length of a rigid-body displacement?, *Mech. Mach. Theory*, **41**, 884–896 (2006).
13. I. Mansouri and M. Ouali, A new homogeneous manipulability measure of robot manipulators based on power concept, *J. Mechatron.* **19**, 927–944 (2009).
14. J.-P. Merlet, Designing a parallel manipulator for a specific workspace, *Int. J. Robotics Res.* **16**, 545–556 (1997).
15. R. Boudreau and C. M. Gosselin, The synthesis of planar parallel manipulators with a genetic algorithm, *J. Mech. Des.* **121**, 533–537 (1999).
16. M. A. Laribi, L. Romdhane and S. Zeghloul, Analysis and dimensional synthesis of the DELTA robot for a prescribed workspace, *Mech. Mach. Theory* **42**, 859–870 (2007).
17. Y. Li and Q. Xu, Optimal kinematic design for a general 3-PRS spatial parallel manipulator based on dexterity and workspace, in: *Proc. 11th Int. Conf. on Machine Design and Production*, Antalya, pp. 571–584 (2004).
18. Q. Xu and Y. Li, Kinematic analysis and optimization of a new compliant parallel micromanipulator, *Int. J. Adv. Robotic Syst.* **3**, 351–358 (2006).
19. B. Siciliano, The Tricept robot: inverse kinematics, manipulability analysis and closed-loop direct kinematics algorithm, *Robotica* **17**, 437–445 (1999).
20. G. Pond and J. A. Carretero, Architecture optimization of three 3-PRS variants for parallel kinematic machining, *Robotics Comp.-Integrat. Manufact.* **25**, 64–72 (2009).
21. D. Zhang and C. M. Gosselin, Kinetostatic analysis and design optimization of the tricept machine tool family, *J. Manufact. Sci. Eng.* **124**, 725–733 (2002).

22. D. I. Kim, W. K. Chung and Y. Youm, Geometrical approach for the workspace of 6-DOF parallel manipulators, in: *Proc. IEEE Int. Conf. on Robotics and Automation*, Albuquerque, NM, pp. 2986–2991 (1997).
23. E. F. Fichter, A Stewart platform based manipulator: general theory and practical consideration, *J. Robotic Res.* **5**, 157–182 (1986).
24. J. A. Carretero, M. A., Nahon and R. P. Podhorodeski, Workspace analysis and optimization of a novel 3-DOF parallel manipulator, *Int. J. Robotics Automat.* **15**, 178–188 (2000).
25. R. E. Stamper, L.-W. Tsai and G. C. Walsh, Optimization of a three DOF translational platform for well-conditioned workspace, in: *Proc. IEEE Int. Conf. on Robotics and Automation*, Albuquerque, NM, vol. 4, pp. 3250–3255 (1997).
26. N. M. Rao and K. M. Rao, Dimensional synthesis of a spatial 3-RPS parallel manipulator for a prescribed range of motion of spherical joints, *Mech. Mach. Theory* **44**, 477–486 (2009).
27. Y. Li and Q. Xu, GA-based multi-objective optimal design of a planar 3-DOF cable-driven parallel manipulator, in: *Proc. IEEE Int. Conf. on Robotics and Biomimetics*, Kunming, pp. 1360–1365 (2006).
28. C. Houck, J. Joines and M. Kay, A genetic algorithm for function optimization: a MATLAB implementation, *Technical Report NCSU-IE-TR-95–09*, North Carolina State University (1995).

About the Authors

Mir Amin Hosseini is currently a PhD student in the Department of Mechanical Engineering, Babol University of Technology. He received his BS in Manufacturing Engineering from Tehran Polytechnic University and MS in Manufacturing Engineering from Tarbiat Modarres University. His research interests focus on parallel machine tools.

Hamid-Reza M. Daniali is currently an Associate Professor in the Department of Mechanical Engineering, Babol University of Technology. He graduated as a Mechanical Engineer at Ferdoosi University, in 1965. He received the MS from Tehran University, in 1968, and the PhD degree in Mechanical Engineering from McGill University, in 1995. His research interests focus on theoretical kinematics and parallel manipulators.

Hamid D. Taghirad is currently an Associate Professor with the Faculty of Electrical and Computer Engineering and the Director of the Advanced Robotics and Automated System Research Center at K. N. Toosi University of Technology, Tehran, Iran. He received his BS degree in Mechanical Engineering from Sharif University of Technology, Tehran, Iran, in 1989, and his MS in Mechanical Engineering, in 1993, and his PhD in Electrical Engineering, in 1997, both from McGill University, Montreal, Canada. He became a Member of the IEEE, in 1995, and a Member of the Board of the Iranian Society of Mechatronics, in 2003. His research interest is robust and nonlinear control applied to robotic systems. His publications include two books, and more than 130 papers in international Journals and conference proceedings.